Technical Note

Development of a Real-time Laser-based Microplatform to Induce Carotid Artery Thrombosis in Rats

Chin-Hsien Chang[1,2,6] Kuo-Ti Chen[6] Yen-Jung Chou[1] Lih-Lian Chen[1]

Tsong-Hai Lee[3] Chao-Hung Wang[4] Ching-Liang Hsieh[5] Yen-Lin Chang[6,*]

[1]*Center for Traditional Chinese Medicine, Chang Gung Memorial Hospital, Keelung 20202, Taiwan, ROC*
[2]*School of Traditional Chinese Medicine, Chang Gung University Taoyuan 33302, Taiwan, ROC*
[3]*Department of Neurology, Chang Gung Memorial Hospital, Linkou Medical Center, Keelung 33378, Taiwan, ROC*
[4]*Department of Cardiology, Chang Gung Memorial Hospital, Keelung 20202, Taiwan, ROC*
[5]*Graduate Institute of Acupuncture Science, China Medical University, Taichung 40402, Taiwan, ROC*
[6]*Department of Biomedical Engineering, Chung Yuan Christian University, Taoyuan 32023, Taiwan, ROC*

Received 5 May 2010; Accepted 21 Jul 2010; doi: 10.5405/jmbe.818

Abstract

The purpose of this study was to develop a novel, laser-based microplatform for inducing carotid artery thrombosis in rats by coupling microscopic recordings and laser inductions on a real-time basis. Our platform model not only provides a direct and precise induction of carotid artery thrombosis in rats at any given time during an experiment but also allows altering the desired experimental parameters over the entire course. We have successfully designed a mild and gradually progressive thrombosis model in an animal. Our model suggests a strong potential usage for studying cerebral embolism caused by cerebral ischemia in near pathological and/or physiological circumstances found in clinical practice which are often not taken into account in current animal models. Therefore, our research model provides a means for clinicians to monitor treatments for their patients with cerebral stroke. Another application of this model is that it can be used to study hemodynamics and its related subjects. Depending on the desired degree of vessel occlusion, we can monitor the experimental parameters such as dosage of photosensizer dyes and intensity of laser light source, etc. This model can serve as a basic research tool for drug development and further development of effective therapeutic regimens in thrombogenesis. In summary, our improved and easy-to-use rat model of laser-induced carotid artery thrombosis has great potential to become more flexible, applicable and practical than previously published animal models.

Keywords: Cerebral stroke, Carotid artery, Thrombosis, Laser, Rat model of thrombosis

1. Introduction

According to the World Health Organization (WHO) statement, "Global Burden of Disease", cerebrovascular disease is the second leading cause of mortality among high-income countries and the fifth among low-income countries [1,2]. Stroke has become a considerable physical, mental and economic burden, making ischemic stroke research an important focus of cerebrovascular research [3,4]. Most cerebral stroke studies were conducted using one of several rat cerebral ischemia models induced by ligation or embolism techniques [5-9]. Ligation requires monitoring and controlling blood pressure, making it a technically challenging method. The embolism method, which uses a foreign substance to block the stroke-related artery, is easy to operate. However, it is poorly controlled and has poor reproducibility.

The use of lasers has found wide application in medicine and biology. Animal models of photochemical-induced thrombosis in studies of cerebral stroke have been developed since the late 1980s. This investigation aimed to refine and improve the current technique. One of the problems observed is the damage of vascular endothelium due to the thermal effect as a result of photochemically induced injury [10-12] Furthermore, the experimental parameter setups in those studies often result in transient formation of thrombosis. We tested different wavelengths of irritation using low intensity to avoid damage in vascular endothelium and to create chronic pathological changes in carotid artery associated with thrombosis.

We incorporated a semiconductor-pumped solid state frequency-doubling green laser [13-17] (diode pumping solid state frequency doubling green laser, hereafter referred to as DPSS Green Laser) at a constant power and diode laser into

* Corresponding author: Yen-Lin Chang
Tel: +886-3-2654505; Fax: +886-3-2654599
E-mail: yenlin@cycu.edu.tw

the optical path of the microscope in order to generate a laser-induced rat carotid artery thrombosis [18] platform together with real-time observation equipment. Thrombosis was induced in the rat carotid artery using lasers in order to improve the traditional rat cerebral ischemia model [19-20] for basic medical research and provide opportunities for clinical research in stroke treatment. Different modes of thrombosis can be generated by different dyes and laser light sources, leading to different embolic circumstances. This study provides a new research platform for the development of novel therapeutic modalities and new drug development.

In the current study, we developed a new platform for laser-induced carotid artery thrombosis in rats [21]. The platform provides a simple rat cerebral ischemia model for basic medical research while allowing clinicians to evaluate stroke therapeutics. The platform uses different dosages of dye and different laser light sources, depending on the mode of carotid artery thrombosis to be induced, and is a new research platform which can be used either for therapeutic modality or for drug development. In addition, the platform established in the current study aims to simultaneously record experimental changes. The development of thrombosis can be evaluated using data processing and image analysis tools. The efficacy of our platform can be evaluated by comparing and analyzing these results with results from chemical-induced thrombosis models [22-24].

2. Materials and methods

2.1 Establishment of a laser-based microplatform for inducing carotid artery thrombosis in rats

A three-tube stereomicroscope (Askania SMC-4, Germany) was used as the microscopic observation equipment and placed on an anatomical platform designed by us. The CCD camera was connected to the original camera output of the microscope. The video signal output was then connected to the storage device and to the monitor. Video signals were saved in standard file format on a computer-readable medium. The monitor was used as an external real-time observation device to simultaneously observe microsurgery and laser irradiation conditions.

We used two different home-made sources of laser for induction. These were: (1) semiconductor-pumped solid-state frequency-doubling green laser (DPSS frequency-doubling green laser): a 200-mW infrared laser diode (808-nm wavelength) was packaged in the TO-18 case with a window cap. After the window cap was removed, the device was directly coupled to a 3% Nd+3: YVO4 (neodymium-doped yttrium vanadate crystal) laser [25] crystal and KTP [26] (potassium titanyl phosphate, KTiOPO4) nonlinear crystal glue body. The 808-nm infrared light initially excited Nd^{+3} free electrons from the lower $^4I_{9/2}$ energy level to the higher $^4F_{5/2}$ energy level. Free electrons were mediated by radiationless transfer to the $^4F_{3/2}$ energy level. This was followed by light emission at a wavelength of 1064 nm via the lasing transition and a fall into the $^4I_{11/2}$ energy level. Free electrons were then mediated by radiationless transfer back to the $^4I_{9/2}$ energy level. The 1064 nm infrared light was passed through the co-resonant cavity formed by two reflection mirrors coated separately with Nd^{+3}: YVO4 and KTP to generate 1064 nm infrared laser. Green laser with a wavelength of 532 nm and a fixed power of 10 mW was generated by passing the 1064 nm infrared laser through the frequency-doubling KTP nonlinear crystal. The laser irradiation spot, the full-width half maximum (FWHM), was a circle with a diameter of 0.6 mm and an energy density of 35 mW/mm^2. The design of the laser is shown in Fig. 1(a). (2) Semiconductor laser [27-34]: the InGaAlP/GaAs red laser diode (wavelength, 650 nm; power, 20 mW) was activated by an auto power control circuit and was driven through a collimating lens with a focus of 6.3 mm in diameter and an effective aperture of 2.0 mm in diameter to render the FWHM of 50% red laser into a circle of 0.6 mm in diameter with an energy density of 35 mW/mm^2. (3) A green-light reflection mirror was placed between the stereomicroscope and 532-nm green laser. A red-light reflection mirror was placed between the stereomicroscope and 650-nm red lasers. The mirrors were installed in the two-axis fine-tuning device. Two laser light spots were overlaid with the window center point of the stereomicroscope, which enabled the synchronized operation of microscopic observation and laser irradiation. The completed system is shown in Fig. 1(b).

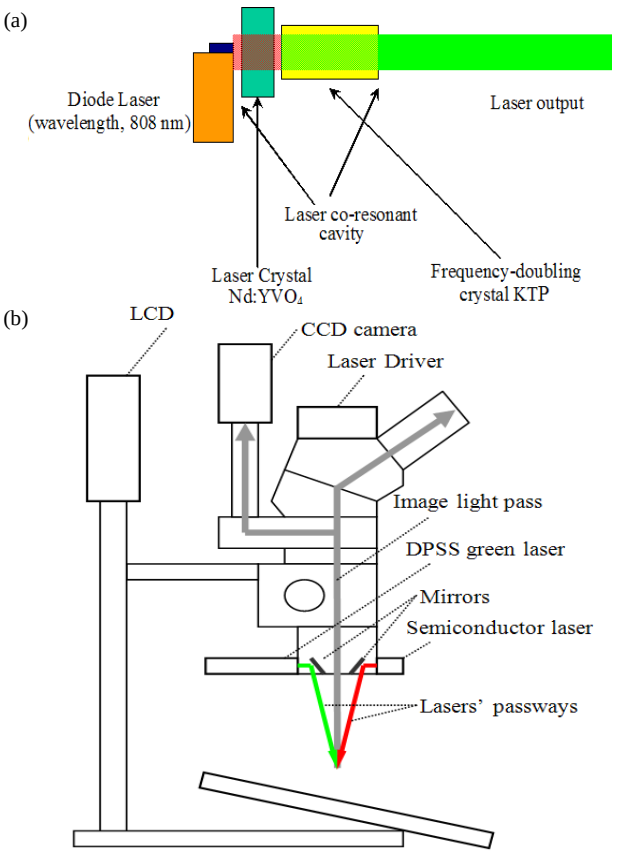

Figure 1. (a) The diagram of a hand-drawn picture showing diode laser, laser crystal. (b) The diagram of a hand-drawn picture of stereomicroscope with indications of LCD, CCD camera.

Wistar–Kyoto (WKY) rats [35-39] (age, 10–13 weeks) were obtained from the National Laboratory Animal Center. Colonies were bred at a controlled temperature (22 ± 0.5°C)

and a relative humidity of 50 ± 10%. The rats were exposed to light for 12–14 h per day and were given ad libitum access to food and water.

For femoral vein annulations and laser-induced thrombosis, the WKY rats were anesthetized and pinned on a surgical board by fixing their legs with rope. The neck skin was incised to find the intersection between the internal and external carotid arteries and the suture was passed under the carotid artery. A skin incision was made near the hip in order to expose the femoral vein. A polyethylene tube (PE 10) was inserted into the left femoral vein. The rat femoral vein was injected with two different photosensitizer dyes: (a) Rose bengal followed by DPSS green laser irradiation of the area 1 cm below the intersection of the external and internal carotid arteries to induce thrombosis, and/then (b) Evans blue followed by laser diode irradiation of the area 1 cm below the intersection of the external and internal carotid arteries to induce thrombosis; (c) The control animals were administered the same amounts of photosensitizer without laser exposure. A complete set-up of this microplatform is shown in Fig. 2.

Figure 2. Development of the laser irradiation microscopic observation platform.

The thigh and neck skin were sutured at the end of the exposure time. Treated rats with ad libitum access to food and water were either continuously bred or sacrificed on the same day (day 0), day 1, week 1, week 3 or week 4. The effect of thrombosis induced by different laser sources and intensity was compared to that in the control animals.

2.2 Effect of different laser powers and dye dosages on thrombosis

Rats were injected with either 30 or 60 mg/kg of rose bengal. DPSS green laser was used as the induction light source, and the exposure times were set as 600, 900, or 1800 seconds. The treated rats were sacrificed on the same day (day 0), day 1, and at weeks 1, 3 and 4. Rats were injected with either 30 or 60 mg/kg of Evans blue. The semiconductor laser was used as the induction light source, and the exposure times were set as 600, 900, or 1800 seconds. The treated rats were sacrificed on the same day (day 0), day 1 and at weeks 1, 3 and 4.

Formation of thrombus in rat models of carotid artery thrombosis is influenced by the injection of different doses of photosensitizer dyes, the exposure to different laser intensity and duration of irradiation. We performed histological analysis to determine the thickness of rat carotid artery as a mean to assess the degree of thrombotic process. Histology was performed as follows. (1) A skin incision was made, and the heart was infused with normal saline to flush out carotid blood. The carotid artery was removed, snap-frozen at -80^{o}C, dissected and subjected to immunohistochemical staining to evaluate proliferation. (2) The carotid artery was frozen for 24 h, and a microtome was used to dissect the carotid arteries (20-μm thick sections) followed by H&E staining. Stained arterial sections were evaluated for thrombosis using the Image-pro Plus 6.0 image analysis software. (3) Vessel occlusion within carotid artery was assessed by immunofluorescence by first antibody (monoclonal mouse anti-SMC actin (1:100)) and secondary antibody (FITC-conjugates goat anti-mouse (1:500)). Tissue was fixed using methanol and PBS-washed. The stained images were examined by laser-scanning confocal microscopy. Images were analyzed and compared using image analysis software. (4) All results were expressed as mean ± SEM. Unpaired *t*-test was used to evaluate differences between the different analytical methods. $p < 0.05$ indicated a statistically significant difference.

3. Results

We developed a novel system for real-time observation, where the site of microsurgery was irradiated by controlled use of two types of lasers (wavelengths of 532 nm and 650 nm). The technique was successfully used to induce the proliferation of rat carotid artery endothelial cells. Our results demonstrated the establishment of a new improvable methodology to induce rat carotid artery thrombosis (Fig. 2). Using this model, control animals that were administered the same amount of photosensitizer dyes, at 4 weeks after day 0 showed no hyperplasia, indicating no thrombotic infarction (Fig. 3).

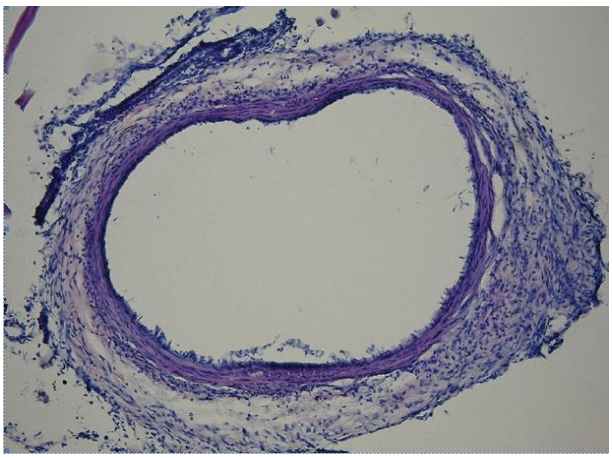

Figure 3. Dissected rat carotid artery endothelium. Endothelial cells did not undergo proliferation.

Rats exposed to 600 seconds of 532-nm DPSS green laser light together with 60 mg/kg rose bengal demonstrated significant hyperplasia in the carotid artery (0.08 ± 0.02 mm) after 28 days (Fig. 4). A weeks after the induction, treated animals started showing a significant increase in proliferation of carotid artery, compared to control animals sacrificed at the

same time. This increase persisted and continued for another 3 weeks. A representative tissue section taken from one of the six rats and stained with H&E showed marked hyperplasia in the carotid artery (Fig. 5(a)). The gray area, possibly some form of thrombotic plug, took up more than 60% of the vascular space in this particular section. All six rats showed a marked increase in hyperplasia and similar histological image. These results were confirmed by immunofluorescence and confocal microscopy (Fig. 5(b)). In contrast, rats that received such treatment and were sacrificed one day after showed no evidence of hyperplasia (data not shown), indicating a mild induction. Together, rats injected with 60 mg/kg rose bengal followed by exposure to 600 seconds of 532-nm DPSS green laser light exhibited a mild and gradual induction of thrombosis over a course of 4 weeks period. Rats treated with 30 mg/kg rose Bengal together with 532-nm DPSS green laser light apparently showed no significant increase in hyperplasia, indicating this dose was too small to induce thrombosis, even with exposure time of 30 minutes (data not shown).

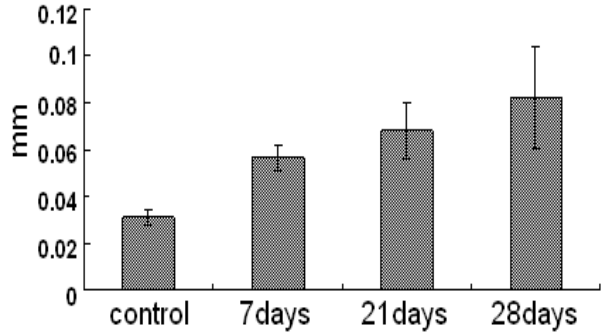

Figure 4. Green laser irradiation for 10 min combined with rose bengal treatment at 60 mg/kg. Optical microscopic observation of induced proliferation of rat arterial wall at different time points. *$p < 0.05$ when compared with the control group, indicating a significant difference (N = 6).

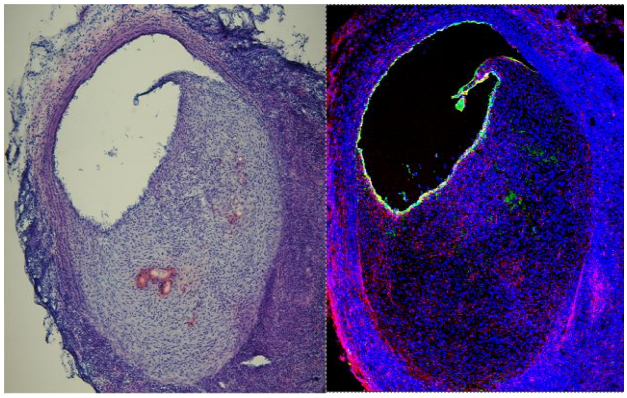

(a) (b)

Figure 5. (a) Representative H&E staining and (b) immunofluorescence staining followed by laser confocal micrography demonstrating significant proliferation in rat carotid artery endothelial cells.

We found no increased proliferation in carotid artery endothelial cells when a laser diode with a wavelength of 650 nm was used as the induction light source, in combination with Evans blue.

4. Discussion

In our current study, we established a laser-induced rat model of carotid artery thrombosis that can be used to create stroke models at different thrombotic degrees by adjusting the duration of laser-induction and dye concentrations. As an added advantage, this model would facilitate basic research on evaluation of stroke treatment. In comparison to the previous experimental parameters of 514 nm, we used a high wavelength of 532 nm, a lower exposure intensity 10 mW, compared to 400 mW and a shorter exposure time of 30 seconds, compared to 10 minutes. Our parameters avoid damage in vascular endothelium and create a flexible animal model of thrombosis closer to the chronic physiological circumstances seen in stroke patients. Our data indicate that using this microplatform, we have successfully created a mild and progressive animal model for photochemically-induced thrombosis. Our data suggest that the formation of vascular thrombosis by injection of rose bengal following DPSS green laser irradiation for four weeks was similar to chronic thrombosis in patients. The absorptive spectrum of rose bengal is relatively narrow, and it is more selective in ranges from 500 nm (blue-green light) to 570 nm (yellow-green light). In contrast, the absorptive spectrum of Evans Blue is relatively broad and is non-selective, with an absorption range from 490 nm (blue light) to 680 nm (red light). Since light absorption is less selective, the response to various wavelengths may be less obvious.

5. Conclusions

The aim of the current study was to investigate the optimal photosensitizer dye and laser irradiation dosage (laser power density and laser irradiation time) for the induction of thrombosis in rat carotid artery. Using our designed platform, we adjusted these experimental parameters and followed the morphological changes in carotid artery under microscope on a real-time basis. Based on the preliminary observations, this study provided evidence that we can further alter parameters that give rise to a desired and/or predicable outcome of thrombogenesis, knowledge that can be widely applied in uncovering the underlying mechanism at early-phase and more progressive stages of the process. Using large-scale genome-wide analysis, one can build a profile composed of morphological changes, metabolite turbulence and genomic alterations in affected tissue at their early phase of thrombogenesis. Knowledge derived from details at cellular and molecular levels will allow the development of a suitable therapeutic regimen for individual stroke patients as well as assist the search for a better drug target in general.

References

[1] C. D. Mathers, T. Boerma and D. MaFat, "Global and regional causes of death," *Br. Med. Bull.*, 92: 7-32, 2009.

[2] A. Zur Nieden, C. Dietz, T. Eikmann, J. Kiefer and C. E. W. Herr, "Physicians appeals on the dangers of mobile

communication: what is the evidence? Assessment of public health data," *Int. J. Hyg. Environ. Health*, 212: 576-587, 2009.

[3] T. J. Quinn and J. Dawson, "Acute 'strokenomics': efficacy and economic analyses of alteplase for acute ischemic stroke," *Expert Rev. Pharmacoecon. Outcomes Res.*, 9: 513-522, 2009.

[4] C. H. Wilkins, J. Mathews and Y. I. Sheline, "Late life depression with cognitive impairment: evaluation and treatment," *Clin. Interv. Aging*, 4: 51-57, 2009.

[5] N. Zhang, N. Miyamoto, R. Tanaka, H. Mochizuki, N. Hattori and T. Urabe, "Activation of tyrosine hydroxylase prevents pneumonia in a rat chronic cerebral hypoperfusion model," *Neuroscience*, 158: 665-672, 2009.

[6] Y. Zhou, N. Fathali, T. Lekic, J. Tang and J. H. Zhang, "Glibenclamide improves neurological function in neonatal hypoxia-ischemia in rats," *Brain Res.*, 1270: 131-139, 2009.

[7] P. Dohare, P. Garg, U. Sharma, N. R. Jagannathan and M. Ray, "Neuroprotective efficacy and therapeutic window of curcuma oil: in rat embolic stroke model," *BMC Complement. Altern. Med.*, 8: 55, 2008.

[8] N. Henninger, B. T. Bratane, B. Bastan, J. Bouley and M. Fisher, "Normobaric hyperoxia and delayed tPA treatment in a rat embolic stroke model," *J. Cereb. Blood Flow Metab.*, 29: 119-129, 2009.

[9] W. W. Zhang, L. Zhang, W. K. Hou, Y. X. Xu, H. Xu, F. C. Lou, Y. Zhang and Q. Wang, "Dynamic expression of glucose transporters 1 and 3 in the brain of diabetic rats with cerebral ischemia reperfusion," *Chin. Med. J.*, 122: 1996-2001, 2009.

[10] B. D. Watson, W. D. Dietrich, R. Prado and M. D. Ginsberg, "Argon laser-induced arterial photothrombosis: characterization and possible application to therapy of arteriovenous malformations," *J. Neurosurg.*, 66: 748-754, 1987.

[11] N. Futrell, B. D. Watson, W. D. Dietrich, R. Prado, C. Millikan and M. D. Ginsberg, "A new model of embolic stroke produced by photochemical injury to the carotid artery in the rat," *Ann. Neurol.*, 23: 251-257, 1988.

[12] W. D. Dietrich, R. Prado, M. Halley and B. D. Watson, "Microvascular and neuronal consequences of common carotid artery thrombosis and platelet embolization in rats," *J. Neuropathol. Exp. Neurol.*, 52: 351-360, 1993.

[13] G. I. Wenzel, S. Balster, K. Zhang, H. H. Lim, U. Reich, O. Massow, H. Lubatschowski, W. Ertmer, T. Lenarz and G. Reuter, "Green laser light activates the inner ear," *J. Biomed. Opt.*, 14: 044007, 2009.

[14] J. U. J. Escudero, E. L. Alcina, M. R. de Campos, F. R. Benlloch, F. S. Ballester and E. M. Vidal, "Green light laser efficacy in patients with prostatic hyperplasia treatment with 5-alpha reductase inhibitors," *Actas Urol. Esp.*, 33: 988-993, 2009.

[15] R. P. C. Lira, A. B. D. M. Calheiros, M. M. V. C. Barbosa, C. V. D. Oliveira, S. L. S. Viana and D. C. Lima, "Efficacy and safety of green laser photocoagulation for threshold retinopathy of prematurity," *Arq. Bras. Oftalmol.*, 71: 49-51, 2008.

[16] V. Krishnakumar, S. Sivakumar and R. Nagalakshmi, "Investigations on the physicochemical properties of the nonlinear optical crystal for blue green laser generation," *Spectrochim. Acta A Mol. Biomol. Spectrosc.*, 71: 119-124, 2008.

[17] D. Chen, Z. Fang, H. Cai, J. Geng and R. Qu, "Instabilities in a grating feedback external cavity semiconductor laser," *Opt. Express*, 16: 17014-17020, 2008.

[18] X. Gao, P. K. Zhi and X. J. Wu, "Low-energy semiconductor laser intranasal irradiation of the blood improves blood coagulation status in normal pregnancy at term," *Journal of Southern Medical University*, 28: 1400-1401, 2008.

[19] C. M. Lim, S. W. Kim, J. Y. Park, C. Kim, S. H. Yoon and J. K. Lee, "Fluoxetine affords robust neuroprotection in the postischemic brain via its anti-inflammatory effect," *J. Neurosci. Res.*, 87: 1037-1045, 2009.

[20] R. Ukai, O. Honmou, K. Harada, K. Houkin, H. Hamada and J. D. Kocsis, "Mesenchymal stem cells derived from peripheral blood protects against ischemia," *J. Neurotrauma*, 24: 508-520, 2007.

[21] N. Futrell, "An improved photochemical model of embolic cerebral infarction in rats," *Stroke*, 22: 225-232, 1991.

[22] M. A. Robinson, D. C. Welsh, D. J. Bickel, J. J. Lynch and E. A. Lyle, "Differential effects of sodium nitroprusside and hydralazine in a rat model of topical FeCl3-induced carotid artery thrombosis," *Thromb. Res.*, 111: 59-64, 2003.

[23] H. Du, J. A. Zawaski, M. W. Gaber and T. M. Chiang, "A recombinant protein and a chemically synthesized peptide containing the active peptides of the platelet collagen receptors inhibit ferric chloride-induced thrombosis in a rat model," *Thromb. Res.*, 121: 419-426, 2007.

[24] S. Lockyer and J. Kambayashi, "Demonstration of flow and platelet dependency in a ferric chloride-induced model of thrombosis," *J. Cardiovasc. Pharmacol.*, 33: 718-725, 1999.

[25] H. Schneckenburger, A. Hendinger, R. Sailer, M. H. Gschwend, W. S. Strauss, M. Bauer and K. Schutze, "Cell viability in optical tweezers: high power red laser diode versus Nd:YAG laser," *J. Biomed. Opt.*, 5: 40-44, 2000.

[26] H. Yanyan, L. Zhengjia, H. Chuyun and Y. Yuncheng, "KTP green laser vaporization of biologic tissue under water and its clinical application," *Photomed. Laser Surg.*, 26: 337-341, 2008.

[27] T. Shimazaki, M. Ishida, T. Tanaka, K. Morimoto, T. Hayashi, S. Degawa and K. Ariyoshi, "A case of endobronchial noncartilaginous hamartoma removed by high-frequency electrosurgical snaring and semiconductor laser," *Journal of the Japanese Respiratory Society*, 48: 108-112, 2010.

[28] X. Yu, T. B. Gibbon, M. Pawlik, S. Blaaberg and I. T. Monroy, "A photonic ultra-wideband pulse generator based on relaxation oscillations of a semiconductor laser," *Opt. Express*, 17: 9680-9687, 2009.

[29] J. G. Wu, G. Q. Xia and Z. M. Wu, "Suppression of time delay signatures of chaotic output in a semiconductor laser with double optical feedback," *Opt. Express*, 17: 20124-20133, 2009.

[30] H. Someya, I. Oowada, H. Okumura, T. Kida and A. Uchida, "Synchronization of bandwidth-enhanced chaos in semiconductor lasers with optical feedback and injection," *Opt. Express*, 17: 19536-19543, 2009.

[31] A. Laurain, M. Myara, G. Beaudoin, I. Sagnes and A. Garnache, "High power single-frequency continuously-tunable compact extended-cavity semiconductor laser," *Opt. Express*, 17: 9503-9508, 2009.

[32] N. Kim, J. Shin, E. Sim, C. W. Lee, D. S. Yee, M. Y. Jeon, Y. Jang and K. H. Park, "Monolithic dual-mode distributed feedback semiconductor laser for tunable continuous-wave terahertz generation," *Opt. Express*, 17: 13851-13859, 2009.

[33] F. K. Khan and D. T. Cassidy, "Widely tunable coupled-cavity semiconductor laser," *Appl. Opt.*, 48: 3809-3817, 2009.

[34] A. Bousseksou, R. Colombelli, A. Babuty, Y. De Wilde, Y. Chassagneux, C. Sirtori, G. Patriarche, G. Beaudoin and I. Sagnes, "A semiconductor laser device for the generation of surface-plasmons upon electrical injection," *Opt. Express*, 17: 9391-9400, 2009.

[35] H. Fujinaka, T. Yamamoto, L. Feng, M. Nameta, G. Garcia, S. Chen, A. A. El-shemi, K. Ohshiro, K. Katsuyama, Y. Yoshida, E. Yaoita and C. B. Wilson, "Anti-perforin antibody treatment ameliorates experimental crescentic glomerulonephritis in WKY rats," *Kidney Int.*, 72: 823-830, 2007.

[36] I. Yaroslavsky and S. M. Tejani-Butt, "Voluntary alcohol consumption alters stress-induced changes in dopamine-2 receptor binding in Wistar-Kyoto rat brain," *Pharmacol. Biochem. Behav.*, 94: 471-476, 2010.

[37] S. M. Gibney, R. D. Gosselin, T. G. Dinan and J. F. Cryan, "Colorectal distension-induced prefrontal cortex activation in the Wistar-Kyoto rat: implications for irritable bowel syndrome," *Neuroscience*, 165: 675-683, 2010.

[38] G. Subramaniam, F. I. Achike and M. R. Mustafa, "Effect of acidosis on the mechanism(s) of insulin-induced vasorelaxation in normal Wistar-Kyoto (WKY) rat aorta," *Regul. Pept.*, 155: 70-75, 2009.

[39] V. Lella, D. Stieber, M. Riviere, J. Szpirer and C. Szpirer, "Mammary cancer resistance and precocious mammary differentiation in the WKY rat: identification of 2 quantitative trait loci," *Int. J. Cancer*, 121: 1738-1743, 2007.